Control Design Profits Heliostat Techno-Economics

Nick Rubin[1], Thomas Roos[2], Fintan Wilson[2], Jason de Villiers[2] and Strinivasan Perumal[2]

1 Systems Engineer – CSIR, P O Box 395, Pretoria, 0001, South Africa, Phone: 0128413383, Fax:0128413179, NRubin@csir.co.za 2 THRoos@csir.co.za, FWilson@csir.co.za, JdVilliers@csir.co.za, SPerumal@csir.co.za

Abstract

Modelling, Identification, Simulation and Synthesis are well known components of the System Engineering Process. Ally these with the Target Aligned (TA) heliostat architecture and the universally acknowledged merits of using closed loop feedback control, then one has all the requisite tools to produce a cost effective solar energy product that can deliver impact in the renewable energy arena.

Keywords: Heliostat; CSP field; position control; cost-benefit tradeoffs

1. Introduction

Roos [1] motivates that the use of heliostat mirrors for solar power concentration, combined with the conversion of thermal to electrical energy via gas turbine, is economically attractive for remote, semi-rural settlements. For reasons of complexity and cost reduction, a single, spheroidal, reflecting mirror is often realized using several mirror panels. The individual mirror panels can be flat section; or may be deformed into spheroidal sections that focus individually at the requisite focal length. Or each section can be formed as that specific section appropriate to its position in the original spheroid (the more complex and expensive option). In the former two cases, the individual sections are canted inwards to focus at the collector plane. Such canting is only accurate for one particular elevation and azimuth solar incidence angle at the mirror centre, at all other incidence angles, aberration defocuses the composite spot from the individual images. Target Aligned heliostats, proposed by Ries et al. [2], have the promise of improving the energy efficiency due to reducing these aberration effects, since the solar incidence angle at the mirror is constrained to lie in the sagittal (pitch) plane of the mirror. On long summer days, Chen et al. [3] estimate the reduction in spillage at the receiver, using TA heliostats, to be between 10 % and 30 % (dependent on receiver area).

This paper reports on the improvements in tracking performance, and the economic impacts associated with reduced spillage at the receiver, that accrue through improved analysis, modelling and design techniques.

2. Background

2.1. Previous Results

It is testimony to the robustness of feedback control that a stabilizing tuning of the two independent, closed loop systems (over the dominant area of the operating envelope) resulted in respectable tracking performance. However stabilisation is merely a necessary attribute of a good control system, further requirements typically also include acceptable regulation performance and disturbance rejection. Previous testing on a 1,25 m² research heliostat by Roos [1] indicated that tracking accuracy in the low milliradian regime was achievable using a Solar Aligned optical sensor and fixed pulse-width ON /OFF control of the pitch and roll axes of the mirror. It is testimony to the robustness of feedback control that a stabilizing tuning of the two independent, closed loop systems (over the dominant area of the operating envelope) resulted in respectable tracking performance.

Work on the planned solar power research field at the CSIR-Pretoria site until now has been done on two proxy heliostats : a 1,25 m^2 experimental heliostat [4] and a prototype 25 m^2 heliostat [1]. A custom-built two-axis controller was initially developed for the experimental heliostat as a project at UKZN, Durban, in

2007. This controller was thereafter modified to also control the prototype 25 m^2 heliostat [5]. With this controller, tracking accuracy in the low milliradian error regime was achievable using a Solar Aligned optical sensor and fixed pulse-width ON /OFF control of the pitch and roll axes of the mirror. The effective proportional gain of these loops had been found by trial and error, by backing off from the point of stability limit, which still gave fairly tight tracking performance for high solar elevation angles, although this simple control law consequently made it susceptible to limit-cycling (amplitude constrained instability) at low solar elevation angles.

3. Design Considerations and Technical Performance

3.1. Updated Controller Design

A controller hardware change was necessitated due to the custom designed hardware, built with the 2007 vintage experimental heliostat, being unmaintainable. Accordingly a COTS two-axis controller module was acquired, which includes dual integrated H-bridge servo drives and over-current and thermal protection.
The upgraded control algorithm was explicitly designed to address actuator backlash, and was implemented using dual control strategies that operate in parallel. The first strategy implements a simple, and so robust, proportional control with significant low pass filtering, to realise good steady state regulation.
The second strategy incorporates a model reference controller which acts to prevent the deleterious effects of backlash. Significant filtering of the optical tracker signals has been introduced, including a sharp notch filter at 50 Hz. The controller cyclic rate is 180 cycles per second, while the ARM core powering the controller has the speed to run the filters at 28’000 filter operations per second.

The actuation commands are retained in the bang-bang format, even though the COTS controller does provide PWM modulation. This being for compatibility with alternative control modules that are currently under development at the CSIR.

3.2. Test Method

Performance was characterised in tests during 2011 (original controller) and 2012 (updated controller). The test modus operandi was identical in both cases. The heliostat was oriented to cast a solar image over a nominal range of 59 m onto the vertical wall of a building, close to perpendicular with respect to the heliostat attitude. A single mirror facet was used, to cast a close to circular solar image. Step, ramp and normal solar tracking tests were performed and recorded by video camera from an average slant range of 11.6 m. The vertical wall had been constructed using rectangular blocks, which acted as a natural, fiduciary, Cartesian grid, which was surveyed using a laser range finder. The local earth co-ordinates of critical blocks were determined by fitting the range data. Where the tests did vary was in the actual video equipment used and the method of analysis.

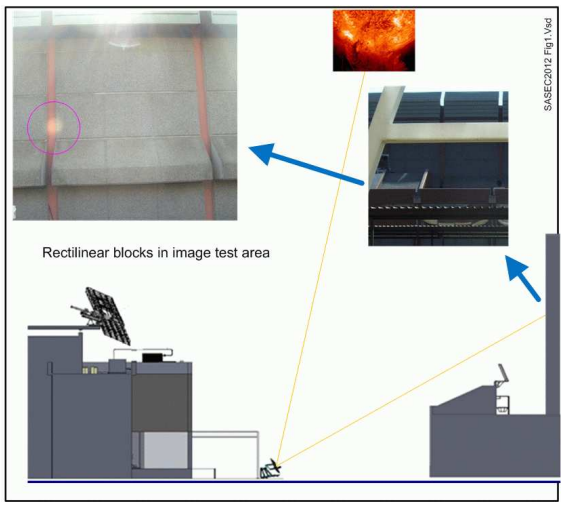

Fig. 1. Heliostat Test Setup

The 2011 tests had the benefit of assistance from the Image Processing group from CSIR Optronics. The image motion was recorded at 20 fps with a 1600x1200 pixel, Prosilica GE1660, video camera using a Schneider Cinegon 4.8mm/f1.4 lens to give an 82° (azimuth) wide angle field of view, with associated, significant lens distortion.
The 2012 tests were recorded at 28 fps with a 640x480 pixel, Pentax E30, digital camera using unknown optics and zoomed to an 18.5° (azimuth) wide angle field of view. This camera has previously been tested and found to have acceptably low distortion of straight horizontal and vertical lines, and is believed to have sufficient internal lens correction methods.

3.3. Results - Original (2007) Controller

The method of wide angle distortion correction is described extensively in [6], suffice it to say here that the primary requirement for correction in this application was that straight lines in the real-world project into straight lines in image space. This new method of distortion correction was evaluated using regular figures prior to processing the recorded data, with impressive results :

Pattern type	Measurement method	Initial distortion (pixels RMS)	Optimal distortion (pixels RMS)
Open CV Calibration[1]		-	0.770
Circle, size 10	Centroid	347.645	0.081
	Ellipse	347.785	0.088
Circle, size 25	Centroid	335.622	0.078
	Ellipse	335.510	0.142

Table. 1. Image Distortion Correction - Results

The image motion was determined by processing each frame as follows. First the frame was de-warped so that orthogonal co-ordinates in the image are also orthogonal in the original scene. Thereafter the solar image on the wall was extracted using a simple threshold filter, and the centroid of this image was calculated. A quality measure of the number of points detected in the solar image was logged. The pitch and azimuth coordinates of the image centre were determined from survey data of the wall, and the time-stamped pitch and azimuth attitude, and centroid quality were output for each frame.
The two camera attitudes were transformed to attitudes with respect to the heliostat optical centre, using survey locations of the camera and heliostat, and the appropriate Polar → Cartesian, translation, Cartesian → Polar operations. The principal measure of performance is the rms deviation of the angle of the centre of the

image from the angle to its mean position during the test. This was compared with the pythagorean combination of the rms deviations of the pitch and azimuth deviations from their mean positions during the test, as this is the underlying method used in HFLCAL.
The main result, indicating the performance of the 2007 vintage controller, is the rms deviation of the total angular displacement :

2007 vintage, stabilizing controller : **σ** (centroid ang. error) = 0.55 mrad

The individual pitch and azimuth rms deviations are

σ (centroid pitch error) = 0.40 mrad **σ** (centroid azim. error) = 0.41 mrad

The pythagorean combination, Sqrt (**σ**^{2}(pitch) + **σ**^{2}(azim)) is

σ (pitch & azimuth) = 0.57 mrad

Figure 2 below indicates the time history of the total angular error (red), pitch error (green), azimuth error (blue) and the quality measure (cyan – note plotting scale factor and offset).

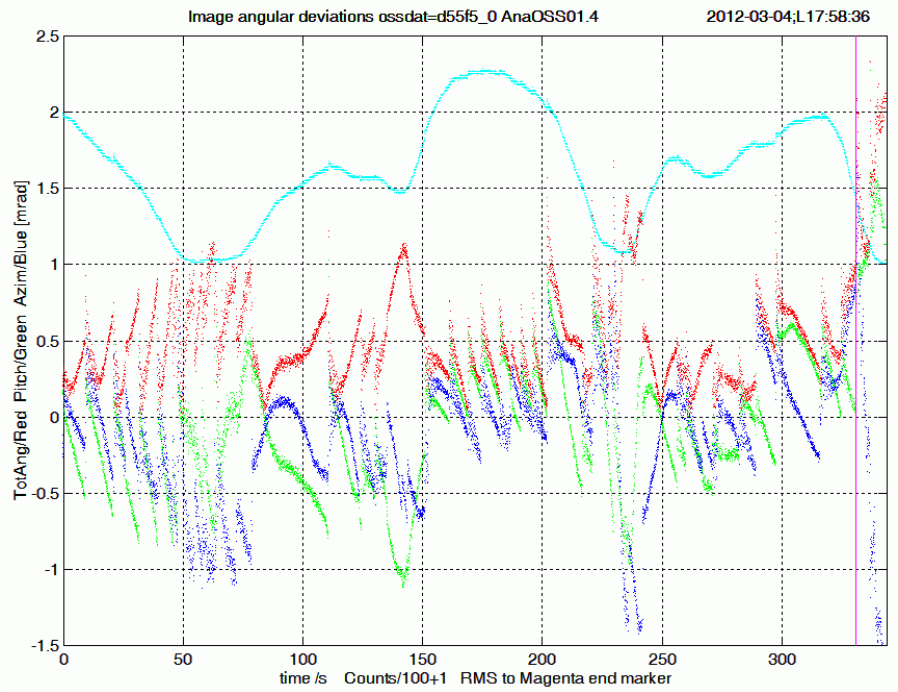

Fig. 2. Angular error deviations for Original Controller

3.4. Results – Updated (2012) Controller

The image motion was determined by visual inspection of each frame during video replay on a PC. Critical frames were captured in an engineering drawing application, and overlayed with a measurement circle concentric with the solar image, and a diagonal across one of the laser surveyed fiduciary blocks in the image. The image coordinates of these graphics were measured with drawing application and the Cartesian location of the solar image centre was thus directly calculated without need to go through equivalent angle from the image centre. Thereafter the same Polar ←→ Cartesian transformations and shifts were used as previously.
The main result, indicating the performance of the 2007 vintage controller, is the rms deviation of the total angular displacement :

Updated controller : σ(centroid ang. error) = 0.26 mrad

The individual pitch and azimuth rms deviations are

σ(centroid pitch error) = 0.14 mrad σ(centroid azim. error) = 0.23 mrad

The pythagorean combination, Sqrt ($\sigma(\text{pitch})^2 + \sigma(\text{azim})^2$) is

σ(pitch & azimuth) = 0.26 mrad

Figure 3 below indicates the time history of the pitch error (red) and azimuth error (green). The total error is dominated by the azimuth error. The blue + symbols indicate the number of frames which the controller was active correcting accumulated error.

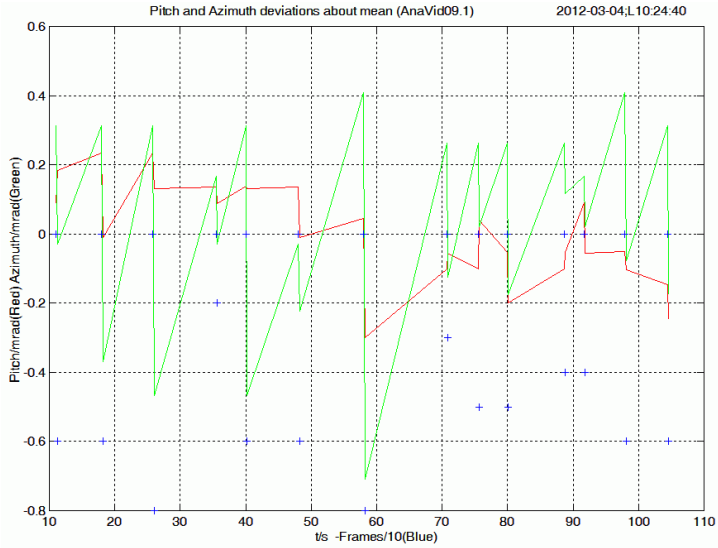

Fig. 3. Angular error deviations for Updated Controller

3.5. Comparison of Controller Performance

The most notable result is that the updated controller has reduced the rms of the total angular error deviation, for the specific test conducted, from 0.57 mrad to 0.26 mrad. The economic impact of this on field capital cost is examined below. The nature of the controller responses is also different. The errors with the original controller indicate far slower frequencies, which will probably translate into sluggish disturbance rejection. In contrast, the responses with the updated controller indicate that the controller invariably changes the sign of the error (around the mean) within 10 to 20 seconds, which will probably mean that with wind or other disturbances it will have superior performance.

4. Economic Impact

4.1. Method of Comparison

DLR [7] performed several preliminary layouts for the CSIR, using HFLCAL acting on the above parameters. These preliminary layouts comprised heliostats arranged in patterns close to circular arcs (rows) in plan view, with these arcs concentric with the receiver. Radially and azimuthally equispaced heliostat arrangements have the advantage of fixed focal lengths within each row, and also reducing the shading and blocking optical interference effects.

Refinements of the layout process, however, perturb the highly symmetrical pattern, as evidenced in the

progression to Figs. 3 and 5 in [7]. The former layout was produced using HFLCAL with circular normal approximations for the main optical and control system effects of solar image losses at the receiver. The true aspect ratio plot indicates strong presence of nine constant radius arcs, and East-West symmetry in the field. It was under these field layout assumptions that a simulation model was developed at the CSIR in 2011, in order to refine the solar spillage models in HFLCAL. The principal improvements in this model were to lift the restrictive assumptions of circular normal distributions for all sources of solar image dispersion, and to replace these with normal distributions in elevation and azimuth. Furthermore a more representative solar intensity distribution was used to determine spillage more accurately, given the distribution in centroid position of the solar image due to other optical and control system effects.

The initial purpose of this model was to undertake a techno-economic study to assess the cost-benefit trade-off to select the number of heliostat mirror section focal lengths, it appeared that the cost versus benefit implications of using either three or four focal lengths was not significant - however this is not the subject of the present article. What the techno-economic model has been used for, in this case, is to look at the cost savings associated with improved tracking performance.

The model uses a strict concentric arc arrangement for the heliostats (so it cannot immediately be used with the layouts produced in Fig. 5 of [7]), and determines the power losses due to spillage. These power losses are related to an economic impact by means of calculating the hypothetical, fractional increase in the number of heliostats to return to the power had there been no spillage losses. A second part of the model determined the costs associated with NRE costs associated with the three vs. four focal length option, and the costs of keeping spares for the different focal lengths – however that is not relevant to the current issue at hand.

4.2. Causes of Spillage

HFLCAL lumps all causes of spillage into a single parameter, the so called Beam Error [7] :

3.987 mrad : beam error (incl. sun shape 2.35 mrad, tracking 0.95 mrad (1 sigma – per axis), slope 1.3 mrad (1 sigma – per axis)).

This is the parameter of a zero mean Circular Normal Distribution. There are other parameters that interact with this parameter, but it embodies all of the effects that cause image spread at the receiver. The economic consequence of the above value for this parameter is compared with what it could be with the current performance of the upgraded controller – two scenarios are considered.

In the first instance, the effect of halving the controller rms error deviation is considered, since that has been observed comparing the original 2007 controller with the 2012 upgrade. Secondly, the figure of 0.95 mrad was provided to DLR based on expectations of tracking regulator performance, encoder sensor accuracy and disturbances – primarily wind and gravity. The present observations are that the total angular rms error (both axes, and including the nett effect on image angular perturbation, not purely error on the mirror normal) corresponds to an equivalent value of 0.13 mrad (1 sigma per axis). What would be the economic impact if that was actually achievable (even in the presence of wind and gravity disturbances)?

4.3. Key results

Table 2 below shows the key technical and economic impacts of the different causes of spillage, using the Beam Error as originally provided to DLR (3.987 mrad).

Field Row	Number of heliostats per field row	Total heliostat collection fraction	Total row collection	Total Heliostat cost per row [€]
1	4	1.000	4.000	13931
2	6	1.000	6.000	20897
3	8	1.000	8.000	27863
4	5	1.000	5.000	17414

5	6	1.000	6.000	20897
6	7	1.000	7.000	24380
7	6	0.979	5.875	20897
8	10	0.943	9.432	34829
9	7	0.904	6.327	24380
TOTAL	59	8.826	57.634	205489
INCREASE				€4872

Table 2. Techno-economic impacts with nominal Beam Error (3.987 mrad)

The *collection fraction* indicates the balance after spillage has been modelled, using individual effects in their respective axes. The *total row collection* relates this to the field layout. The relative shortfall between the total row collection and the number of heliostats is multiplied by the total field cost to obtain the effective economic impact of spillage, in this case nearly 5'000 Euros.
Table 3 below shows the changes in total collection and the decrease in economic losses of spillage should the tracking error be halved from 0.95 to 0.475 mrad (since the upgraded controller appears likely to achieve a halving in rms tracking error), and then further decreased to a hypothetical level prompted by the upgraded controller performance. It is apparent that the law of diminishing returns would apply if the tracking error could be reduced to, what is by all accounts, a dramatically small tracking error.

Field Row	Total row collection 0.475 mrad		Total row collection 0.13 mrad
1	4.000		4.000
2	6.000		6.000
3	8.000		8.000
4	5.000		5.000
5	6.000		6.000
6	7.000		7.000
7	5.939		5.957
8	9.626		9.682
9	6.497		6.546
TOTAL	58.061		58.185
INCREASE	€3322		€2880

Table 3. Techno-economic impacts with tracking error halved and with further reduction

Conclusions

This paper reports on the improvements in image pointing performance of a Target Aligned heliostat that have been realised through an upgraded tracking controller. This improvement has been related to the reduction in economic cost of spillage, with a ballpark figure of 1500 Euros in capital expenditure on a 59 heliostat field, which certainly exceeds the cost of the upgraded controller hardware.

Acknowledgements

This work was supported and funded by the Council for Scientific and Industrial Research.

References

[1] Roos, T., et al., 25 m^2 Target-Aligned Heliostat with Closed-Loop Control, SES Solar World Congress 2007: Solar Energy and Human Settlement, Beijing, China, 18-21 September 2007

[2] Ries, H., Schubnell, M., The Optics of a Two-Stage Solar Furnace, Solar Energy Materials, 21 (1990)

[3] Chen, Y., et al., Comparison of Two Sun Tracking Methods in the Application of Heliostat Field, Journal of Solar Energy Engineering 126 (2004)

[4] Maliage, M., Roos, T., The Distribution from a 1,25 m^2 Target Aligned Heliostat: Comparison of Ray Tracing and Experimental Results, submitted to SASEC2012, 21-23 May 2012, Stellenbosch

[5] Roos T., Buck R., Pfahl A., Design of a Multi-Purpose Target-Aligned Heliostat Field, Proceedings ISES SWC 2009, 11-14 October 2009, Johannesburg

[6] de Villiers, J., Wilson, F., Nicolls, F., The effects of Lens Distortion Calibration Patterns on the Accuracy of Monocular 3D Measurements, PRASA2011, Proc. 22nd Ann. Symp. Pattern Recognition Soc. SA

[7] Buck, R., Pfahl, A., Roos, T., Target Aligned Heliostat Field Layout for Non-Flat Terrain, submitted to SASEC2012, 21-23 May 2012, Stellenbosch